Tanzania Journal of Engineering and Technology 2022, **41(2)**:1-15

Websites: https://www.ajol.info/index.php/tjet, https://tjet.udsm.ac.tz

ISSN 1821-536X (**print**); ISSN 2619-8789 (**electronic**)
DOI: 10.52339/tjet.v41i2.775

Full Length Research Paper

28 GHz Patch Antenna Array with Reduced Mutual Coupling for 5G Communications Systems

Rahabu F. Mwang'amba and Hashimu U. Iddi*

Department of Electronics and Telecommunications Engineering, College of Information and Communication Technologies, University of Dar es Salaam

*Corresponding author: rahabu80@gmail.com and hashimuledi@udsm.ac.tz

ABSTRACT

A 28 GHz patch antenna array with reduced mutual coupling for 5G communication systems is presented in this paper. Two elements antenna array was simulated with a periodic boundary to represent an infinity array. The antenna array is attached with a pair of the coupled directional coupler with a coupling value of -3.47 dB, and transmission lengths of 3.40 mm and 7.62 mm depending on the antenna array's magnitude and phase coefficient were designed and simulated. A reduced mutual coupling of -31.86 dB compared to -10.75 dB for an array without a decoupling network was observed. The wide scanning angle of ±180° was also achieved. These results were obtained under smaller antenna elements interspacing of 0.43λ_0. Moreover, the proposed antenna array design achieved a 3.32 GHz enhanced fractional bandwidth which is 11.8%. Generally, this work found that the combinatorial advantages of using the gap coupled inset feed technique and employing a pair of directional couplers develop the patch antenna array design with better performance.

ARTICLE INFO

Submitted: **December 23, 2021**

First revision: **March 26, 2022**

Second revision: **April 11, 2022**

Accepted: **April 15, 2022**

Published: **June 30, 2022**

Keywords: *Patch Antenna Array, Mutual Coupling, Scanning Angle, 5G, Directional Coupler, and Gap Coupled Inset Feed.*

INTRODUCTION

Antennas operating at millimetre wave (mm-wave) frequencies with bandwidth availability are a promising area for 5G communications, which is not yet extensively explored. These bands can offer enough bandwidth; however, it suffers a high propagation loss *(*Federico *et al.*, 2021; Mehdi *et al.*, 2020*)*. Several studies proposed antennas with high gain to combat the high propagation loss, which necessitates antenna arrays (Qu *et al.*, 2020, Koul *et al.*, 2018). The antenna elements in the arrays produce mutual coupling between them. If their interspacing is less than half wavelength at the resonance frequency (λ_0), it reduces the admittance, resulting in a reduced scanning angle of the antenna (Hansen, 1998; Xia *et al.*, 2015).

Different methods to reduce mutual coupling using isolated elements have been proposed (Cheng & Luo, 2021; Dhamankar & Lopes, 2016). Electromagnetic Band Gap (EBG), which involves introducing the dielectric material on the antenna array, is one of the methods detailed in Vikrant (2013). The EBG suppresses the surface wave in an array by allowing multiple reflections between the patches and dielectric material, producing multiple radiators and gaining enhancement and mutual coupling reduction. However, the introduced dielectric increases the size of antenna arrays (Dellaoui *et al.*, 2018). In Benykhlef (2017), the author proposed an EBG structure with a reduced size of 67.2% compared to the conventional EBG. It achieved a mutual coupling reduction of 6 dB, which is relatively small for large antenna arrays. Defected Ground Structures (DGS), which modifies the ground plane by introducing slots at antenna array ground to reduce mutual coupling between antenna elements, is amongst the other method (Saada, 2017). The DGS defects disturb the current distribution and change the transmission line characteristics such as capacitance and inductance, changing antenna performance (Xia *et al.*, 2015). Apart from reducing mutual coupling, the introduced patterns of slots on the ground can cause severe backward radiation, which can destroy the performance of an antenna array by increasing the back lobe level (Cheng & Luo, 2021; Kiani-kharaji *et al*., 2018). Strongly coupled elements technique is also proposed to provide a good scanning angle, resulting in broadband-enabled antenna elements. This technique can provide a wide scanning angle and compact geometry because it does not need additional structures. Though, the arrangement of the array elements and the distance between the elements remains an interesting area of research (Pralon *et al.*, 2017).

Antennas for 5G must have a gain of at least 12 dB and a bandwidth of more than 1 GHz with a scanning angle ability of at least $\pm 60^0$ (Federico *et al.*, 2021; Sulyman *et al.*, 2014). Some techniques meet the requirements at the expense of increasing the antenna size, so the optimal design needs to consider the bandwidth, gain, antenna element spacing and scanning angle. The scanning ability relies on each antenna element's amplitude and phase, which combine in complex weight to improve sidelobe suppression (Rahimian *et al.*, 2017). This work focused on designing the 28 GHz patch antenna array with reduced mutual coupling for wide scanning ability. Mutual coupling reduction originates from the applied designed pair of directional couplers, which provide indirect coupling for cancelling out with direct mutual coupling from an antenna array. The motive behind the designed decoupling network was to ensure a wide scanning angle by providing wide impedance matching. This work also implied the gap coupled inset feed technique for bandwidth enhancement during the single element antenna design.

METHODS AND MATERIALS

Single Element Antenna Design Process

A single element antenna resonating at 28 GHz was designed and simulated using CST Microwave Studio, and the optimal design was projected into two antenna element arrays. A directional coupler was also designed according to the coupling magnitude and phase of the antenna array for mutual coupling reduction. The initial design of a single element antenna came from the microstrip antenna design equations as detailed in Hansen, (1998), Matin, (2015), Saada, (2017), which obeys the transmission model. The transmission model was chosen because it is easier to get the impedance matching which is very important in ensuring a wide scanning angle. The antenna and directional couplers were designed using Rogers RT 5880 substrate with dielectric constant (ε_r) equals 2.20 since the substrates with low dielectric constant produce microstrip antennas with high bandwidth, which is an essential requirement in antenna for 5G communications systems. The design also used 0.381 mm as the height of substrate (h), which is a thin substrate for antenna miniaturisation, and it is at the accepted range for substrate height, $0.003\lambda_o \leq h \leq 0.05\lambda_o$ (Yazdani, 2008). The initial design comprising the single antenna element with the inset feed technique showed a bandwidth of 0.85 GHz. The gap coupled inset feed technique was employed to obtain a bandwidth of greater than 1 GHz. This technique is one of the feeding techniques used in microstrip patch antenna. It consists of a gap between the feed and the antenna patch, as illustrated in its gap discontinuity π-equivalent circuit in Figure 1.

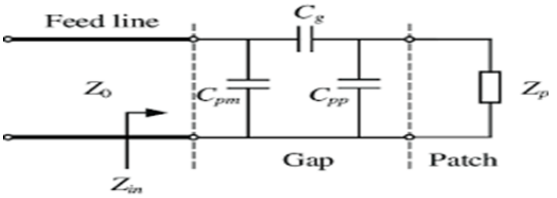

Figure 1: Equivalent circuit of the gap coupled inset feed (Saada, (2017)

Hong & Lancaster (2001) expressed the mathematical equations for estimating the coupling gap capacitance, C_g, for circuit matching. Those equations were evaluated in this work using MATLAB software for estimating the value of gap capacitance, C_g, used to match with the gap size. The introduced gap between the patch and the feed must be properly etched because the abrupt changes in the feed's dimensions may give rise to a change in electric and magnetic field distributions, thereby leading to a direct impact on the antenna reflection coefficient. The C_g reduces with the increase in coupling gap length, $L_{coupled}$, as shown in Figure 2. The study by Martel *et al*, (1991) demonstrated that for infinite gap spacing, C_g approaches zero and C_{pp} equals to the end capacitance for an open ended microstrip line. Hence the open circuit λ/2 microstrip line shunt capacitance was assumed in estimating the initial value for coupling gap capacitance using the following expression:

$C_g = \dfrac{1}{4fZ_o}$ leading to C_g =0.178 *pF*.

When the feed is indirectly connected to the patch, it produces a capacitive circuit. If the gap increases, the source might fail to reach the targeted feeding location at the patch, hence the impedance mismatch. Therefore, the effect of changing the size of the introduced gap had been studied, as shown in Figure 3. The frequency response matched at the gap $L_{coupled}$ = 0.1 mm resulted in an enhanced bandwidth whereby at 28 GHz frequency, the return loss of less than -60 dB was observed, and it deteriorates when the size of the gap changes.

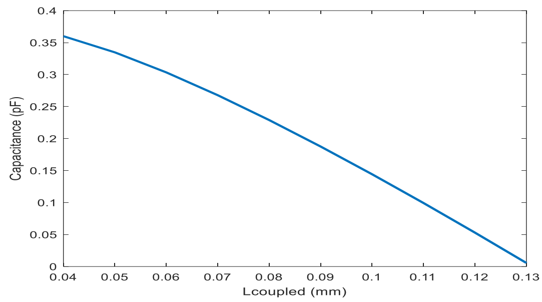

Figure 2: The coupling gap capacitance change with its length

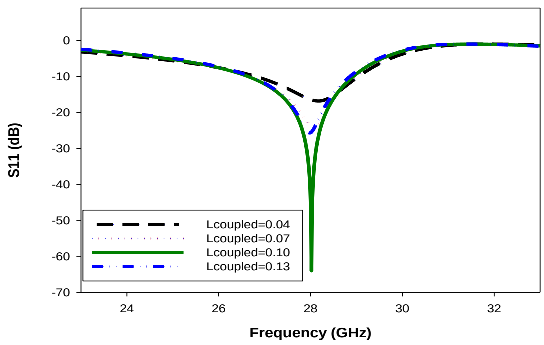

Figure 3: Effect of changing the size of the introduced gap between feed and patch

Performance characteristics like bandwidth, return loss, gain, and directivity are important in designing a single antenna element. These factors affect the overall performance of the antenna array system, so it is necessary to make sure that the designed single antenna element has good performance for the intended application as other factors might not be altered even when extending to an array. The final geometry of a single antenna element was as presented in Figure 4. The optimal values of patch length, width and size of the single element antenna at all are summarised in Table 1.

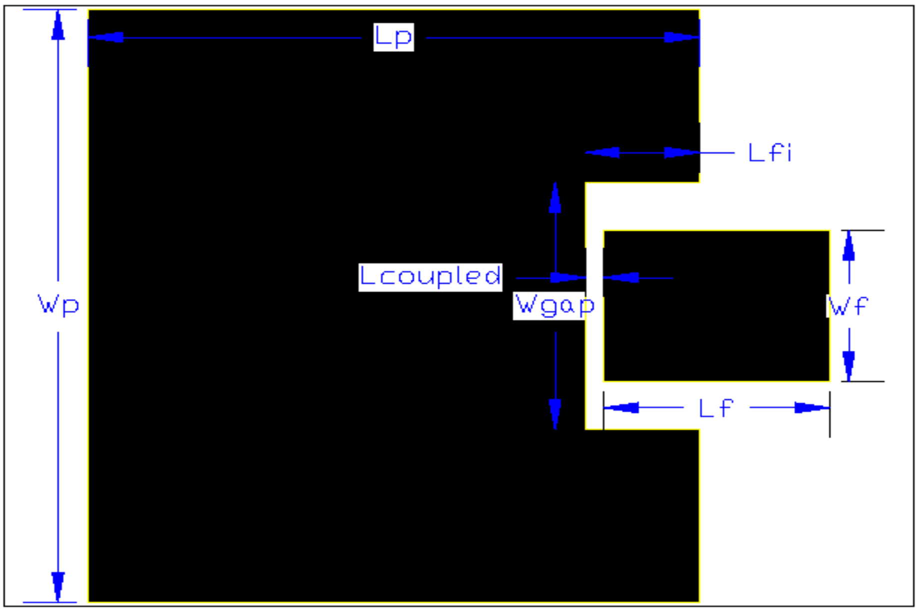

Figure 4: The geometry of the single element antenna

Table 1: Single Antenna element parameters used for simulation

Notation	Value (mm)
L_p	3.200
W_p	3.600
l	0.500
h	0.381
t	0.035
W_f	0.920
L_f	0.680
W_{gap}	1.500
L_{fi}	0.600
$L_{coupled}$	0.100

Antenna Array

A linear structure with varying distances between the patches, *d*, was employed in the geometry of an array because the linear structure tends to keep wide beams orthogonal, thus requiring only 1-D for a wide scanning angle which is very important in 5G handsets. The array indicated that the distance between antenna elements influences the mutual coupling (S_{12}) between them and thus, affects the overall active reflection coefficient (S_{11}) of an antenna array. The proposed two-element antenna array showed the effect of mutual coupling to the interspacing between patch elements, as summarised in Figure 5. The coupling at 28 GHz was very strong when interspacing of d = 1 mm = $0.43\lambda_0$ was considered, and it gives S_{12} of -10.75 dB while it decreases to -25 dB at d = 8 mm = $1.08\lambda_0$.

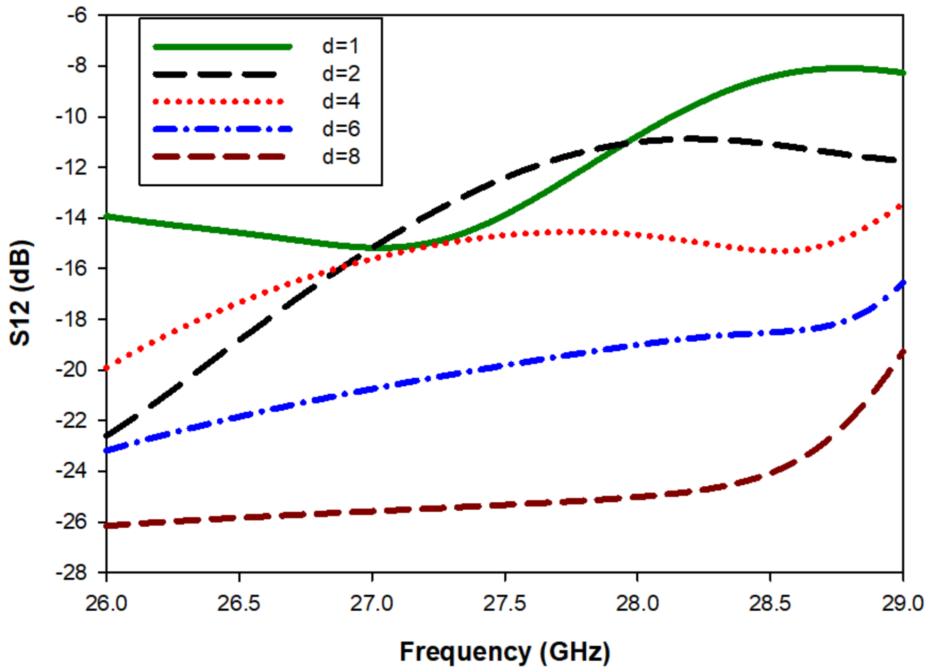

Figure 5: Effect of varying interspacing between antenna elements of an array

Decoupling Network Scattering Matrix

The four-port directional coupler was considered as detailed in Figure 6, including input, isolation, through and coupled. A single directional coupler that is matched and reciprocal has a scattering matrix (Sc) with parameters as shown in (1).

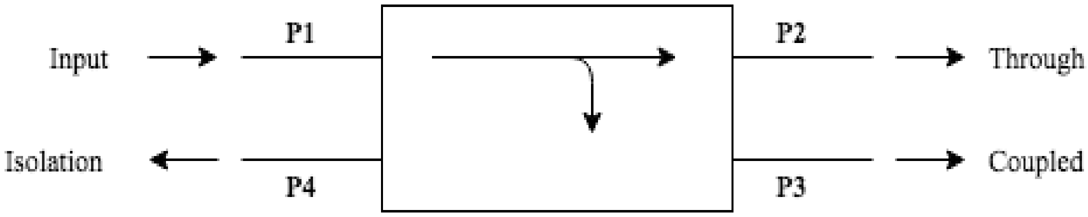

Figure 6: The structuree of a directional coupler

$$S_c = \begin{bmatrix} 0 & S_{c12} & S_{c13} & S_{c14} \\ S_{c21} & 0 & S_{c23} & S_{c24} \\ S_{c31} & S_{c32} & 0 & S_{c34} \\ S_{c41} & S_{c42} & S_{c43} & 0 \end{bmatrix} \tag{1}$$

$$\begin{bmatrix} 0 & S_{c12} & S_{c13} & 0 \\ S_{c12} & 0 & 0 & S_{c24} \\ S_{c13} & 0 & 0 & S_{c34} \\ 0 & S_{c24} & S_{c34} & 0 \end{bmatrix} \begin{bmatrix} 0 & S_{c12} & S_{c13} & 0 \\ S_{c12} & 0 & 0 & S_{c24} \\ S_{c13} & 0 & 0 & S_{c34} \\ 0 & S_{c24} & S_{c34} & 0 \end{bmatrix} = \begin{bmatrix} 1 & 0 & 0 & 0 \\ 0 & 1 & 0 & 0 \\ 0 & 0 & 1 & 0 \\ 0 & 0 & 0 & 1 \end{bmatrix} \tag{2}$$

By unitary property SS* = 1(2), and if $S_{c14} = S_{c23} = 0$ for the directional coupler, the self-product of the rows of unitary property yields a series of equations well derived in (Sierra, 2010).

Sierra (2010) stated that comparing the equations implies that $S_{c13} = S_{c24}$ and $S_{c12} = S_{c34}$ which is always employed in a single coupler only. If a pair of the directional couplers have to be used, then $S_{c12} \neq S_{c34}$ $S_{c12} \neq S_{c34}$ and the scattering matrix of the pair of the directional coupler, S_D, will be expressed as (3). Its scattering parameter elements are detailed (Xia et al., 2015)

$$S_D = \begin{bmatrix} 0 & S_{D12} & S_{D13} & 0 \\ S_{D21} & 0 & 0 & S_{D13} \\ S_{D13} & 0 & 0 & S_{c34} \\ 0 & S_{D13} & S_{D34} & 0 \end{bmatrix} \qquad (3)$$

To ensure decoupling, ideally the value of the total coupling coefficient of decoupling network and antenna array, S_T S_T, was assumed to be zero, which means cancellation of mutual coupling. This gave (4), which is useful in the initial estimation of amplitude of coupling coefficient of decoupling network, C_o. The phase of coupling coefficient of an antenna array, θ_1, was used to estimate the electrical transmission length, L_{t1} $Lt1$, of the decoupling network as per (5).

$$C_0 = \sqrt{\frac{2|S_A|}{1+|S_A|}} \qquad (4)$$

$$\theta_1 = -L_{t1} \qquad (5)$$

From the antenna array, the coupling magnitude, S_A, and phase, θ_1, at interspacing $0.43\lambda_0$ were found to be -10.75 dB and -166.4^0, respectively. By using (4), the coupling magnitude, C_o, of the directional coupler had to be -3.47 dB and the length of transmission line 1, L_{t1} had to be 166.4^o in reference to (5), which is equivalent to 4.95 mm in electrical length. By using the relationship $\theta_1 + \theta_2 = (2n-1)\pi$ for $n = 1, 2, 3$, the length of transmission line 2 was assumed to be 373.6^0, which is equivalent to 11.11 mm electrical length. To comply with the geometry of the designed patch antenna array, which has the $W_p = 3.6$ mm, the ratio 1:2.24 was used as a reference to get L_{t1} and L_{t2} which fits the array geometry.

After designing the pair of directional couplers, the impact of changing distance between coupler lines was investigated in Figure 7. At 28 GHz, distance (s) has little influence on coupler coupling, which can be explained by the fact that this design is grounded on the length of transmission lines in controlling coupler coupling ability. However, $s = 0.1$ mm was chosen in this work as it is within the required accepted range $0.1 \leq s/h \leq 5$ as in (Sierra, 2010) and it gives nearly the calculated value of coupling -3.47 dB.

Also, the distance between coupled lines fixed to s=0.1 mm and the effect of varying width of the coupler (W_c) was studied as shown in Figure 8. It is observed that coupling increases as W_c decreases. After several parametric studies during simulations, the value of W_c equal to 0.7 mm was preferred as it gives the calculated value of coupling and is within the acceptable range. The final structure of the pair of coupled directional couplers is as in Figure 9.

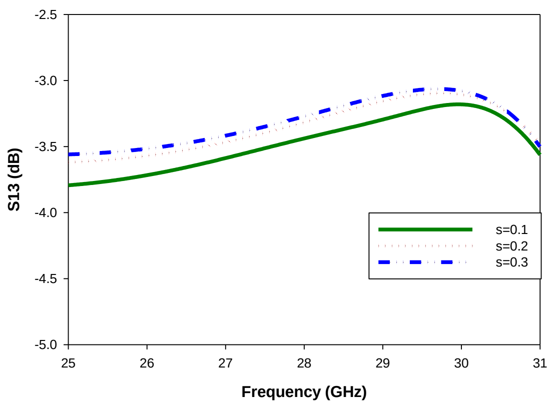

Figure 7: Effect of changing distance between coupler lines of the directional couplers

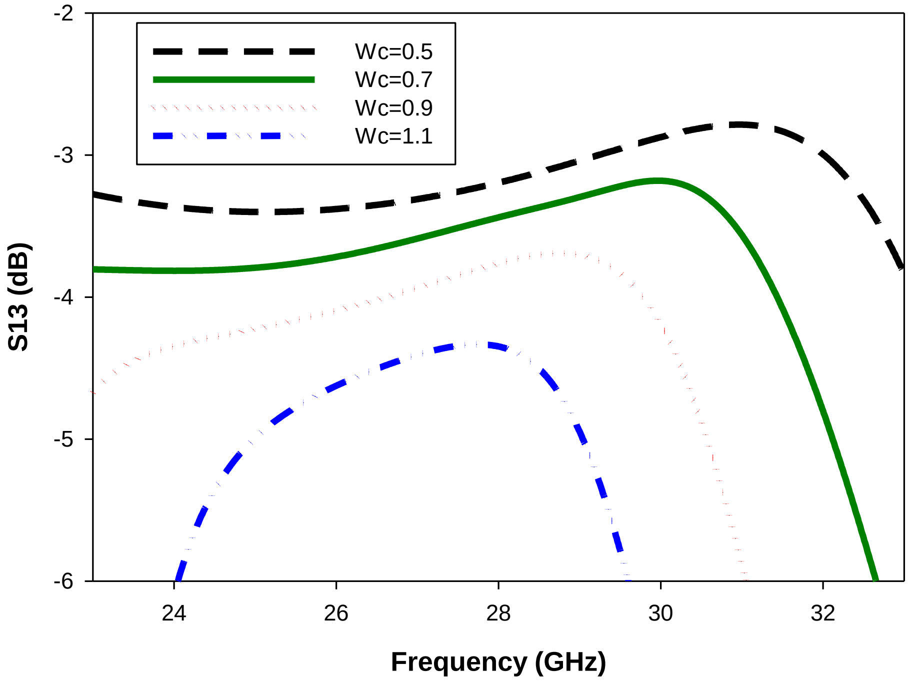

Figure 8: Effect of changing the width of couplers lines

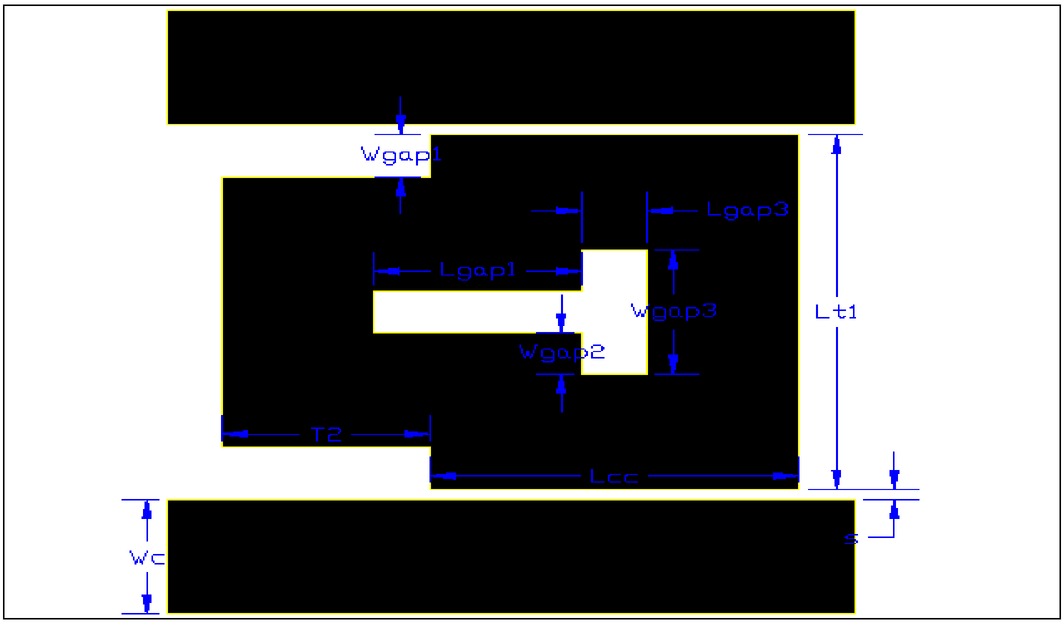

Figure 9: The geometry of the proposed pair of directional couplers

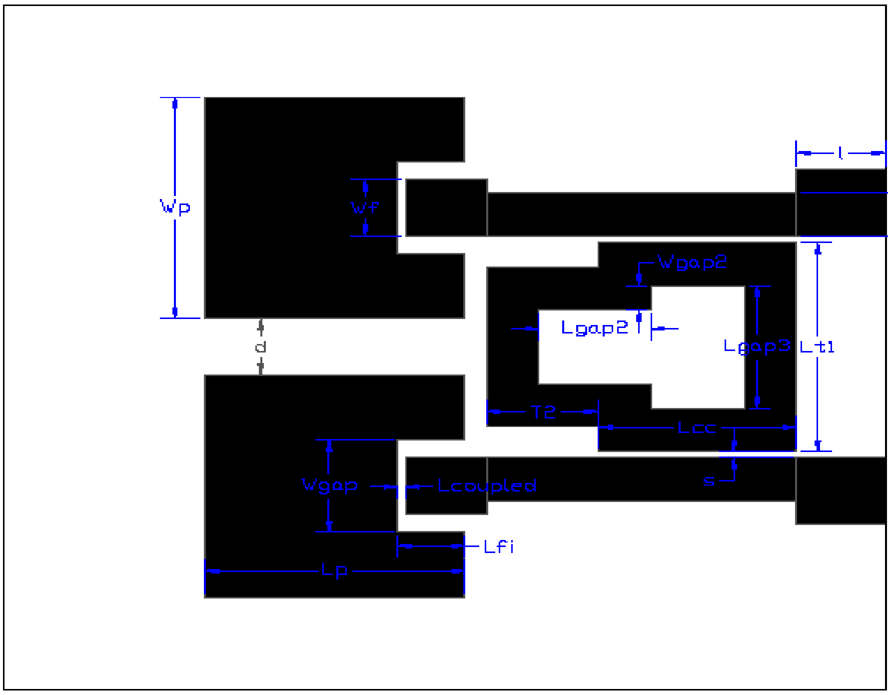

Figure 10: The two-element antenna array integrated with a pair of directional couplers

The decoupling network consists of the optimal design of pair of coupled directional couplers and two antenna element array was integrated and their geometry was arranged as in Figure 10. The optimal values of coupler and two element antenna arrays at all are summarized in Table 2. The detailed performance of this system is analyzed in the next section.

Table 2: Couplers and two element antenna array parameters

Notation	**Value (mm)**
L_{t1}	3.400
L_{cc}	2.670
T_2	1.500
L_{gap3}	2.000
W_{gap2}	1.200
L_{gap2}	1.570
W_{gap2}	0.400
W_{gap1}	0.400
l	1.200
s	0.100
W_c	0.700
d	1.000

RESULTS AND DISCUSSION

Single Element Antenna Return Loss and Bandwidth

The parametric study came up with an optimal return loss value, as shown in Figure 11. The antenna with inset feed indicated a return loss value of -35.1 dB with a bandwidth of 0.85 GHz. After introducing a coupled gap between a patch and feed line that aimed to maintain the input impedance matching, the return loss decreases to -63.5 dB. What cannot be underestimated here is the increase in bandwidth to 2.27 GHz, which is better than other works, as summarised in Table 3. This wide bandwidth is much required in the 5G communication systems. In Halaoui et al, (2020), the antenna element at 28 GHz shows a return loss of -35 dB but with a quite low bandwidth of 0.89 GHz. It uses the inset feeding technique but without gap coupled. Saada, (2017) utilises a gap coupled technique at 28 GHz operating frequency but achieved a bandwidth of 1.245 GHz with a gap coupled of 0.1 mm. The work by Merlin Teresa & Umamaheswari, (2020) presented a compact slotted single element antenna with a bandwidth of 2.02 GHz but with a gain of 6.37 dBi, which is slightly low compared to the 6.63 dBi of this work.

Table 3: Comparison of return losses for single element antenna

Design	**Bandwidth (GHz)**	**Feeding Technique**
Halaoui et al, (2020)	0.89	Inset feed
Saada, (2017)	1.25	Gap coupled inset feed
Merlin Teresa & Umamaheswari, (2020)	2.02	Inset feed with slots
The proposed	2.27	Gap coupled inset feed

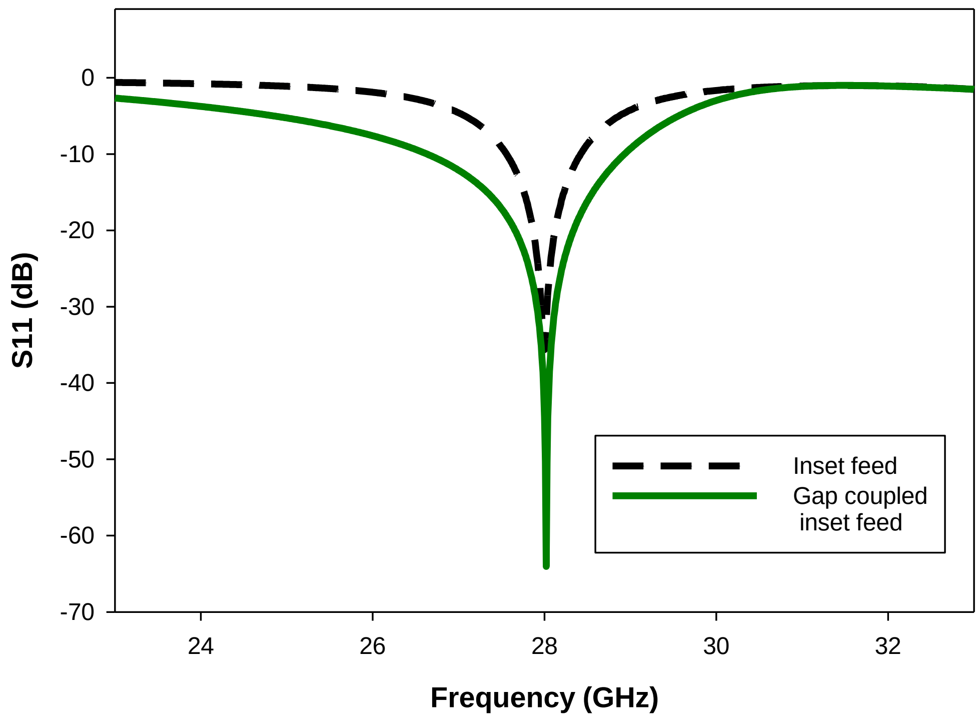

Figure 11: S_{11} results for the antenna with inset feed and gap coupled inset feed

Single Element Antenna Radiation Pattern

Figure 12 shows the radiation pattern of an antenna element at 28 GHz in its polar form when *Phi* = 90°. The figure indicates that the directivity of 6.63 dBi with an angular width of 92^0 and the side lobe amount of -12.7 dB was obtained. The wide beamwidth archived is very important as it can lead to a wide scanning angle with less complexity of the whole antenna system (Ahn et al., 2019).

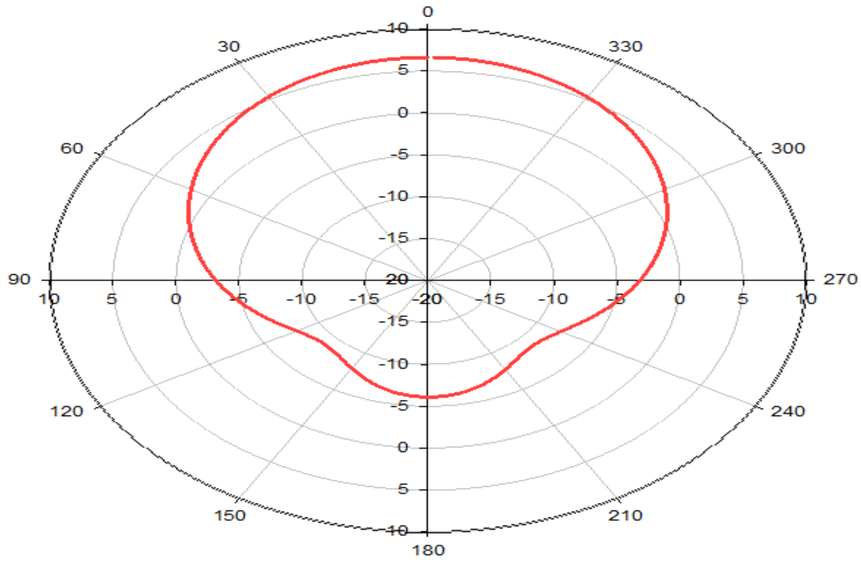

Figure 12: Radiation Pattern of single element antenna

Performance Characteristic of an Antenna Array

The antenna array with a distance of separation *d* =1 mm was chosen as an optimal design. At this distance, the centre-to-centre separation (interspacing) between patches was $0.43\lambda_0$. The bandwidth and return loss are summarized in Figure 13 where a bandwidth of 1.7 GHz was observed at *RL* = -10 dB in which the lowest return loss was -31.5 dB at a scanning angle of 0^o. The gain was also examined by considering an increase in the number of antenna elements from 2 to 16. For two elements and 16 elements, assuming linear geometry, the gain was 8.64 dBi and 17 dBi, respectively.

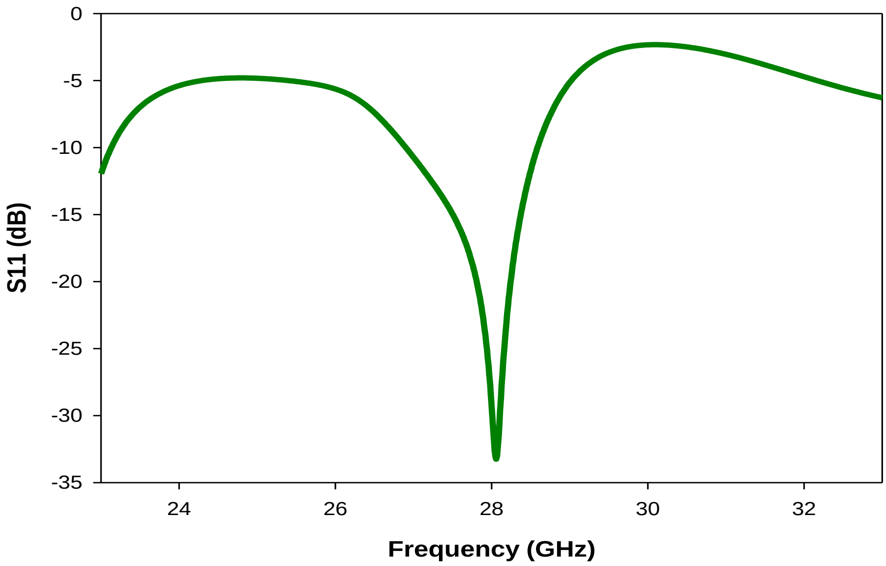

Figure 13: S11 result of a two-element antenna array

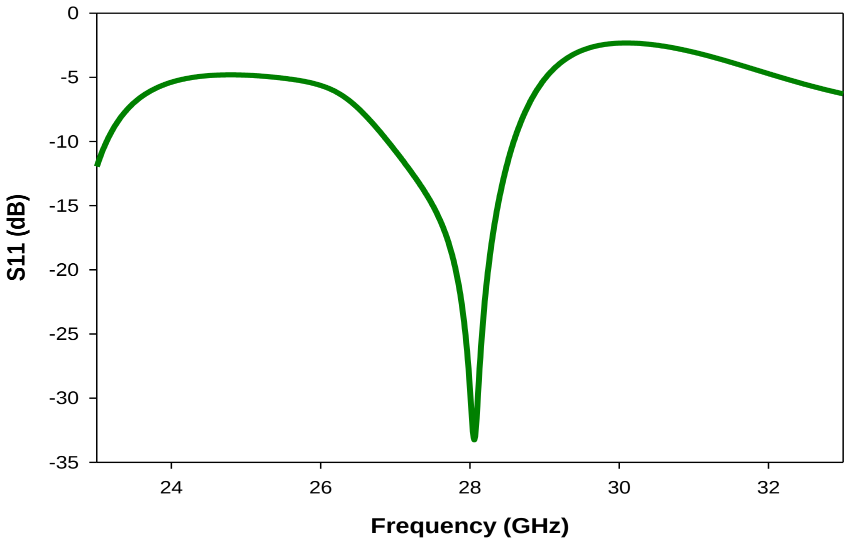

Figure 13: S11 result of a two-element antenna array

Bandwidth of an Antenna Array with Changing Scanning Angle

The periodic boundary was set in the Y direction to investigate the scanning angle of an antenna. The array performance is shown in Figure 14, whereby an increase in scanning angle affects the antenna bandwidth. The antenna array bandwidth at *Theta* = 0^o was 1.7 GHz, but it deteriorated to 0.98 GHz, equivalent to only 3.5% fractional bandwidth, throughout the $\pm 80^0$ scanning angle. At an angle of 40^0, the antenna array resonance frequency highly deviates from the 28 GHz frequency, decreasing the total antenna bandwidth. This deviation is due to variation of impedance matching with change in scanning angle.

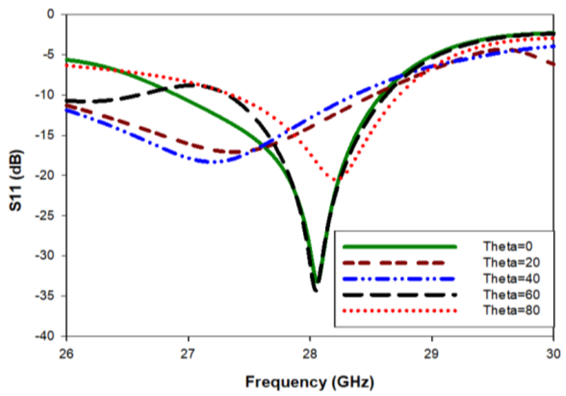

Figure 14: S_{11} varies with scanning angle for two elements antenna array.

Mutual Coupling of Proposed Antenna

When integrated with a pair of directional couplers, the simulated two-elements antenna array demonstrated an improved S_{12} magnitude to -31.9 dB compared to that without the decoupling network with the same antenna element interspacing, which had S_{12} magnitude of -10.75 dB as shown in Figure 15. This reduction resulted from the cancelation of the mutual coupling between the antenna elements with the coupling from the directional coupler. This approximately 20 dB reduction of mutual coupling within the operating frequency greatly influences the creation of wide-angle impedance matching, which is amongst the important criteria in antennas for 5G communication systems.

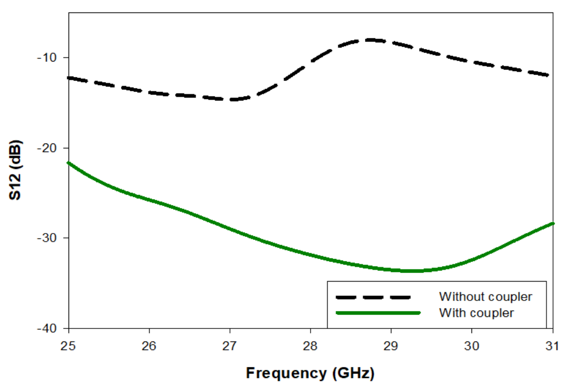

Figure 15: Coupling magnitude of the antenna array with and without decoupling network.

Proposed Antenna Scanning Angle

The studied scanning angle shows that for scanning angle up to $\pm 80^{0}$, the antenna system return loss is less than -10dB, which implies that the simulated antenna system shows a scanning angle $\pm 80^{0}$ as shown in Figure 16. The directional coupler employed to reduce mutual coupling between antenna elements has also enhanced the bandwidth of an antenna array as compared to that of an antenna array without the decoupling network from 2.27 GHz to 3.32 GHz. This is because as wide-angle impedance matching is achieved, the antenna maintains the active reflection coefficient at a wider frequency band. In analysing the simulation results of the designed antenna system, the return loss (S_{11}) was examined. Referencing to ITU standards for communications systems in 5G, less than -10 dB is required to avoid mismatch. In this design, the return loss value of less than -10 dB was observed throughout the scanning angles of $\pm 80^{0}$ with a maximum value of 1.21 at 28 GHz frequency. The value of S_{11} achieved signifies that the reflected power at the antenna ports is low. Hence, the antenna and transmission line are perfectly matched.

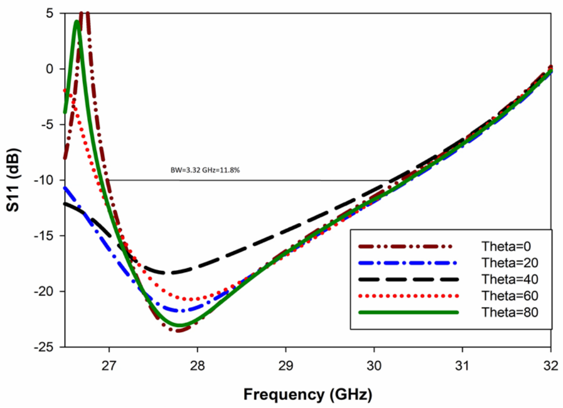

Figure 16: The scanning angle of a designed antenna system.

Performance Characteristics of the Designed Antenna System

The overall performance of the complete antenna array and coupler had a bandwidth of 3.32 GHz with reduced mutual coupling to -31.86 dB. A good directivity of 8.59 dBi was observed considering only two-element antenna arrays. However, the gain increases as the number of elements increases, whereby 4 and 8 element antenna arrays returned 11.6 dB and 14.8 dB gain, which are relatively better compared to other related works with the same number of antenna elements. Table 4 summarises the performance of the designed patch antenna array compared to the existing related works for 28 GHz in terms of interspacing and scanning angle.

Table 4: Interspacing and scanning angle comparison of the proposed design with other related studies

Design	Interspacing (mm)	Scanning angle
Koul et al. (2018)	$0.50\lambda_0$	64^{0}
Ahn et al, (2019)	$0.90\lambda_0$	70^{0}
Mehdi et al, (2020)	$0.52\lambda_0$	$\pm 80^{0}$
The Proposed Antenna	$0.43\lambda_0$	$\pm 80^{0}$

It can be observed from Table 3 that the proposed antenna system performs better than compared to the existing related works for 28 GHz. It achieved the wide scanning angle at the small antenna interspacing which match well with the antenna miniaturisation idea.

CONCLUSION

This paper proposed the 28 GHz patch antenna array with gap coupled inset feed and a pair of directional couplers as the decoupling network. A single element antenna shows improvement of bandwidth from 0.89 GHz using inset feed technique to 2.27 GHz when gap coupled inset feed technique was employed. This work also presents the reduced mutual coupling network using a pair of directional

couplers, showing mutual coupling reduction from -10.75 dB to -31.86 dB compared to the antenna array without a decoupling network. The reduced mutual coupling was obtained under the smaller antenna elements interspacing of $0.43\lambda_0$.
Additionally, the proposed 28 GHz patch antenna array system achieved a wide scanning angle of $\pm 80^0$. On top of that, the proposed antenna array design indicated an enhanced bandwidth of 3.32 GHz which is 11.8%. Generally, this found that the combinatorial advantages of using the gap coupled inset feed technique and employing a pair of directional couplers develop the patch antenna array design with better performance.
The further improvement in mutual coupling might enhance the bandwidth as wide bandwidth is vital for 5G antennas which might be achieved by proper utilization of some bandwidth enhancement techniques like slotting.

REFERENCE

Ahn, B., Hwang, I., Kim, K., Chae, S., & Yu, J. (2019). Wide-Angle Scanning Phased Array Antenna using High Gain Pattern Reconfigurable Antenna Elements. *Scientific Reports*, 1–13. https://doi.org/10.1038/s41598-019-54120-2

Alsager, A. F. (2011). Design and Analysis of Microstrip Patch Antenna Arrays. *Unpublished Masters Thesis, University College of Boras, Sweden*, *1*, 1–80.

Attia, H. (2019). Highly reduced mutual coupling between wideband patch antenna array using multiresonance EBG structure and defective ground surface. *Microwave and Optical Technology*, *September*, 1–10. https://doi.org/10.1002/mop.32193

Benykhlef, F. (2017). EBG Structures for Reduction of Mutual Coupling in Patch Antennas Arrays. *Journal of Communication Software and Systems*, *13*(1), 9–14. https://doi.org/10.24138/jcomss.v13i1.242

Cheng, C., & Luo, L. (2021). Mutual Coupling Reduction Using Improved Dual-Layer Mushroom and E-Shaped Stub. *International Journal of Antennas and Propagation*, *2021*. https://doi.org/10.1155/2021/8862570

Dellaoui, S., Kaabal, A., Halaoui, M. El, & Asselman, A. (2018). Patch array antenna with high gain using EBG superstrate for future Patch array antenna with high gain using EBG superstrate for future cellular networks 5G cellular networks Costing models capacity .*Procedia Manufacturing*, *22*, 463–467. https://doi.org/10.1016/j.promfg.2018.03.071

Dhamankar, S., & Lopes, S. (2016b). Mutual Coupling Reduction Techniques in Microstrip Patch Antennas: a Survey. *International Research Journal of Engineering and Technology*, 3, 1064–1069. www.irjet.net

Ellgardt, A. (2009). Wide-angle scanning wide-band phased array antennas. *Unpublished PhD Thesis, KTH University, Sweden*

Federico, G., Caratelli, D., Theis, G., & Smolders, A. B. (2021). A Review of Antenna Array Technologies for Point-to-Point and Point-to-Multipoint Wireless Communications at Millimeter-Wave Frequencies. *International Journal of Antennas and Propagation*, *2021*. https://doi.org/10.1155/2021/5559765

Feng, W., Li, Y., Jin, D., Su, L., & Chen, S. (2016). Millimetre-Wave Backhaul for 5G Networks: Challenges and Solutions. 1–17. https://doi.org/10.3390/s16060892

Ghosh, S., Member, S., Sen, D., & Member, S. (2019). An Inclusive Survey on Array Antenna Design for Millimeter-Wave Communications. *IEEE Access*, *7*, 83137–83161. https://doi.org/10.1109/ACCESS.2019.2924805

Halaoui, M. El, Canale, L., Asselman, A., & Zissis, G. (2020). Dual-Band 28 / 38 GHz Inverted-F Array Antenna for Fifth Generation Mobile Applications †. *International Conference INTER-ENG 2020 Interdisciplinarity in Engineering,*.

Hansen, R. (1998). Phased Array Antennas (K. Chang (ed.); Vol. 9). John Wiley & Sons, Inc. https://doi.org/10.1002/0471224219

Hong, J., & Lancaster, M. J. (2001). Microstrip Filters for RF / Microwave (Vol. 7). JOHN WILEY & SONS, INC. 96.

Hu, C., Chang, D., Yu, C., Hsaio, T., & Lin, D.

(2016). Millimeter-Wave Microstrip Antenna Array Design and an Adaptive Algorithm for Future 5G Wireless Communication Systems. *2016*.

Khan, J. (2008). Design of Microstrip Patch Antenna on Liquid Crystal Polymer (LCP) for Applications at 70GHz. *Polymer*, *September*.

Kiani-kharaji, M., Hassani, H. R., & Mohammad-ali-nezhad, S. (2018). *Wide scan phased array patch antenna with mutual coupling reduction*. 1–7. https://doi.org/10.1049/iet-map.2018.0155

Koul, S. K., Wani, Z., & Abegaonkar, M. (2018). Millimeter-wave antenna with wide-scan angle radiation characteristics for MIMO applications. *International Journal of RF and Microwave Compute=-Aided Engineering*, *July*, 1–9. https://doi.org/10.1002/mmce.21564

Lundvall,A.(2016). Ericsson Mobility Report. *https://www.google.com/url?client=internal-element-cse&cx=partner-pub-4357510538660394:7831812009&q=https://www.abc.es/gestordocumental/uploads/internacional/EMR_June_2016_D5%25201.pdf&sa=U&ved=2ahUKEwicluriqo3zAhVEJhoKHT5eD7MQFnoECAkQAg&usg=AOvVaw31bF2DvSGxempihOPfgC_p*. June.

Martel, J., Boix, R. R., & Horno, M. (1991). Static Analysis of Microstrip Discontinuities Using the Excess Charge Density in the Spectral Domain. *IEEE Transactions on Microwave Theory and Techniques*, *39*(9), 1623–1631. https://doi.org/10.1109/22.83839

Matin, M. A. (2015). A Design Rule for Inset-fed Rectangular Microstrip Patch Antenna 2 Basic Characteristics of Microstrip Patch. *WSEAS Transactions on Communications*, *January 2010*.

Matzner, H., Levy, S., & Ackerman, D. (2009). Experiment 5 Coupler Design. *https://www.google.com/url?client=internal-element-cse&cx=partner-pub-4357510538660394:7831812009&q=https://www.hit.ac.il/.upload/engineering/microwave_-_experiment_5_-_coupler_design.pdf&sa=U&ved=2ahUKEwip-fG9rI3zAhVByxoKHdPRBvUQFnoECAIQAQ&usg=AOvVaw0QutK3XjJ6x6LqXevn6o0S* .June.

Mehdi, M., Taheri, S., Abdipour, A., Zhang, S., & Pedersen, G. F. (2020). Millimeter-Wave Wide Scan Beam Steering 5G MIMO Antenna Array in Mobile Terminals. *14th European Conference on Antennas and Propagation* (EuCAP), 5–9.

Merlin Teresa, P., & Umamaheswari, G. (2020). Compact Slotted Microstrip Antenna for 5G Applications Operating at 28 GHz. *IETE Journal of Research*, *0*(0), 1–8. https://doi.org/10.1080/03772063.2020.1779620

Nalini, K., Suneel, A. S. A. I., & Sridevi, S. B. (2013). E-Shape Patch Antenna for Millimeter Wave Communication. *International Journal of Engineering Sciences Research, IJESR*, Vol. 4, Special Issue 1, 1199–1207.

Pralon, M., Thom, R., Pompeo, B., Beltrao, G., & Pralon, L. (2017). On the Effects of Decoupling and Matching Networks in Phase Array Radiation Patterns for Radar Applications. *IEEE Transactions on Microwave Theory and Techniques*, *1*, 969–972. https://doi.org/10.1109/TMTT.2006.874874

Pramono, S. (2018). Mutual Coupling Reduction & Bandwidth Enhancement Using a Simple Folded Slot-Partial Ground Plane in Dualband MIMO Antenna. *2018 International Seminar on Intelligent Technology and Its Applications (ISITIA)*, 19–22. https://doi.org/10.1109/ISITIA.2018.8711213

Pujol, F., Manero, C., Carle, B., & Remis, S. (2021). 5G Observatory Quarterly Report 11 Up to March 2021. *The European Commission DG Communications Networks, Content & Technology*, 1–117.

Qu, Z., Qu, S., Member, S., Zhang, Z., Yang, S., & Member, S. (2020). Wide-Angle Scanning Lens at 28 GHz Fed by Antenna Array. *IEEE Transactions on Antenna and Propagation*, *c*, 1–8. https://doi.org/10.1109/TAP.2020.2967086

Rahimian, A., Alfadhl, Y., & Alomainy, A. (2017). Design and Performance Analysis of Millimetre-Wave Rotman Lens-Based Array Beamforming Networks for Large-Scale Antenna Subsystems. *Progress In Electromagnetics Research*, *78*(July), 159–171.

https://doi.org/10.2528/PIERC17071703

Rajagopal, S., Abu-surra, S., Pi, Z., & Khan, F. (2011). Antenna Array Design for Multi-Gbps mmWave Mobile Broadband Communication. *IEEE Globecom 2011 Proceedings,* 9–14. https://doi.org/10.1109/GLOCOM.2011.6133699

Saada, M. H. A. (2017). Design of Efficient Millimeter Wave Planar Antennas for 5G Communication systems. *Unpublished Masters Thesis The Islamic University–Gaza*

Sajjad, H., Khan, S., & Arvas, E. (2017). Mutual Coupling Reduction in Array Elements Using EBG Structures.*International Appllied Computational Electromagnetics Society Symposium.* https://doi.org/10.23919/ROPACES.2017.7916410 ,1–2.

Sierra, C. S. S. (2010). Microwave directional couplers. *Unpublished Masters Thesis University of Brescia*

Sulyman, A., Nassar, A., Samimi, M., Maccartney, G., Rappaport, T., & Alsanie, A. (2014). Radio propagation path loss models for 5G cellular networks in the 28 GHZ and 38 GHZ millimeter-wave bands. *IEEE Communications Magazine*, *52*(9), 78–86. https://doi.org/10.1109/MCOM.2014.6894456

Uchendu, I., & Kelly, J. (2016). Survey of Beam Steering Techniques Available for Millimeter Wave Applications. *Progress in Electromagnetics Research*, *68*(March), 35–54.

Vikrant, A. (2013). A Comparison in the Performance of Microstrip patch Antenna with and without EBG Substrate and Superstrate. *Nal Conference on Advanced Computing & Communication Technologies 2012 Third International Conference on Advanced Computing & Communication Technologies*, 150–154. https://doi.org/10.1109/ACCT.2013.35

Xia, R., Qu, S., Li, P., & Yang, D. (2015). Wide-Angle Scanning Phased Array Using an Efficient Decoupling Network. *IEEE Transactions on Antenna and Propagation*, *63*(11), 5161–5165.

Yazdani, T. M. (2008). Design and Fabrication of a Micro-Strip Antenna for Wi-Max Applications. *Unpublished Masters Thesis, Blekinge Institute of Technology,* Sweden